

NASA Technical Memorandum **107656**

11N-14
118084
P-28

IMPROVED HIRAP FLIGHT CALIBRATION TECHNIQUE

Christina D. Moats

Robert C. Blanchard

Kevin T. Larman

N92-33112

Unclas

G3/19 0118084

July 1992



National Aeronautics and
Space Administration

Langley Research Center
Hampton, Virginia 23665

(NASA-TM-107656) IMPROVED HIRAP
FLIGHT CALIBRATION TECHNIQUE
(NASA) 28 p

IMPROVED HIRAP FLIGHT CALIBRATION TECHNIQUE

Christina D. Moats
Lockheed Engineering & Sciences Company
Hampton, Virginia 23666-1339

Robert C. Blanchard
NASA Langley Research Center
Hampton, Virginia 23665-5225

and

Kevin T. Larman
Lockheed Engineering & Sciences Company
Hampton, Virginia 23666-1339

Abstract

A method of removing non-aerodynamic acceleration signals and calibrating the High Resolution Accelerometer Package (HiRAP) has been developed and improved. Twelve HiRAP mission data sets have been analyzed applying the improved in-flight calibration technique. The application of flight calibration factors to the data sets from these missions produced calibrated acceleration levels within $\pm 5.7 \mu g$ of zero during a time in-flight when the acceleration level was known to be less than $1 \mu g$. To validate the current in-flight calibration technique, the atmospheric density results, specifically the normal-to-axial density ratios, have been compared with the analysis results obtained with the previous in-flight calibration technique. This comparison shows an improvement (up to 12.4 percent per flight) in the density ratio when the updated in-flight calibration technique is used.

Nomenclature

A	= acceleration measurements, μg
α	= angle of attack
B	= sensor bias
b	= bias coefficient, μg
cx	= axial aerodynamic coefficient
cz	= normal aerodynamic coefficient
g	= 9.80665 m/s^2 , Earth gravitational constant
Hz	= cycles/sec
M	= temperature coefficient, $\mu g/^{\circ}F$
T	= sensor temperature
μg	= $1 \times 10^{-6} g$
X, Z	= HiRAP sensor location or Orbiter X and Z body axes
ΔA	= incremental acceleration

Acronyms

APU	= Auxiliary Power Unit
GMT	= Greenwich Mean Time
HiRAP	= High Resolution Accelerometer Package
OV	= Orbiter Vehicle
OEX	= Orbiter Experiments
STS	= Space Transportation System

Subscripts

c	= calibrated
f	= flight
o	= reference or initial
u	= due to APU

Introduction

The High Resolution Accelerometer Package (HiRAP) experiment, as part of the NASA Orbiter Experiments (OEX) program, has to date made low-frequency, low-acceleration flight measurements during 12 Space Transportation System (STS) missions. The HiRAP is a tri-axial, orthogonal system of gas-damped accelerometers with a resolution of $1 \times 10^{-6} \text{ g}$ ($1 \mu\text{g}$). The HiRAP mission is to measure low-frequency aerodynamic accelerations. With these measurements, atmospheric density and the aerodynamic flight performance characteristics of the Orbiter Vehicle (OV) can be determined (1).

Orbital and reentry aerodynamic analyses require calibrated low-frequency, low-acceleration measurements. Many flight programs rely upon ground calibrations of the accelerometer instrument system in a 1g environment to properly adjust the μg environment flight measurements. However, experience indicates that ground calibrations have an accuracy within $\pm 100 \mu\text{g}$ (or greater) of zero during a time in flight when the acceleration level is generally accepted to be less than $1 \mu\text{g}$ (2). Until true, in-flight calibration station corrected accelerometry is perfected (3), an alternate method of calibration is necessary.

This paper presents an updated in-flight calibration method used to calibrate HiRAP's low-frequency, low-acceleration data on 12 missions. Also, presented are the results of a direct comparison between atmospheric density ratios produced by the previously used calibration technique and the in-flight calibration technique presented here.

Analysis of Flight Data

The HiRAP science and housekeeping data are recorded in counts as a function of Greenwich Mean Time (GMT). The science data are comprised of acceleration measurements for each of the 3 sensors. The data are

collected at a rate of 174 Hz for all flights except STS-61C, STS-35, and STS-40, which are collected at a rate of 112.7 Hz. The housekeeping data includes measurements of sensor temperature and power supply voltages. The data are recorded at a rate of 1.6 Hz for STS-61C, STS-35, and STS-40, and at a rate of 2.7 Hz for all other flights. The method used to convert the acceleration count values to engineering units is presented in Ref. 1. To obtain an aerodynamic data set, all non-aerodynamic accelerations must be removed. The procedures for removing the effects of thrust induced accelerations and rotational induced linear accelerations, caused by the instrument offset from OV center of gravity, are documented in Refs. 1 and 2. After thrust removal and center-of-gravity adjustments have been made, a 1-sec average is made of the acceleration data. Since the averaged data set represents the acceleration data, due only to aerodynamic accelerations and bias, the data set is ready for calibration.

Flight Calibration

The first step in the flight calibration method is to determine an OV altitude, at which aerodynamic acceleration levels are less than $1 \mu g$. The model and current flight calibration technique used are presented in Ref. 2. For STS-07, the model predicts accelerations of less than $1 \mu g$ above 227 km and 214 km, respectively, for the X- and Z-axes. The uncalibrated acceleration data and the selected calibration intervals are shown in Fig. 1. The calibration parameters for each flight are presented in Table I. The linear regression of sensor acceleration with sensor temperature produces a bias calibration of the form

$$B_{fi} = M_i (T_i - T_{oi}) + b_i$$

where $i = X, Z$. The bias slope and intercepts of the linear regression, as well as the associated uncertainty estimates, are presented in Table II. The method for obtaining the calibration uncertainty estimates is documented in Ref. 2. These uncertainty estimates are evaluated over the calibration sensor temperature range to obtain the maximum orbital acceleration measurement uncertainties presented in Table III. As shown, the flight calibration acceleration levels have an accuracy within $\pm 5.7 \mu g$ of zero. Table IV, the maximum reentry acceleration measurement uncertainties, is an evaluation of the uncertainty estimates over the range from sensor temperature at calibration to sensor temperature at sensor saturation. The flight calibration acceleration levels have an accuracy within $\pm 26.4 \mu g$ of zero at a measurement of $-8000 \mu g$. The bias value, B_{fi} , resulting from the linear regression is removed from the uncalibrated aerodynamic data using:

$$A_{ci} = A_i - B_{fi}$$

where $i = X, Z$. The resulting aerodynamic accelerations, presented for STS-07 in Figs. 2 and 3, are very near zero during the calibration interval.

As detailed in Ref. 2, the three Auxiliary Power Unit (APU) exhaust ports are located at the tail of the OV. The thrust from these ports is manifested as an acceleration signal shift, shown in Fig. 3, on the Z-axis only. The acceleration increment due to the APU, ΔA is determined by evaluating both the pre- and post- APU calibration intervals at the location of the APU transition. To complete the bias determination for the Z-axis data, the post-APU acceleration shift is incorporated into the bias calibration factors previously determined. The bias determination for the Z-axis data following the last APU transition becomes:

$$A_{cz} = A_z - B_{fz} + \Delta A_{uz}$$

where ΔA is the change in acceleration due to the APU. For STS-07, the calibrated Z-axis acceleration data, which includes the correction for $\Delta A_{uz}=40 \mu g$, is presented in Fig. 4.

Atmospheric Density Ratio Results

A previous analysis (Ref. 1) details the aerodynamic coefficient model. The same model was used with updates for the axial, $c_x(\alpha)$, and normal, $c_z(\alpha)$, aerodynamic coefficients at 40° angle of attack. For this analysis, $c_x(\alpha)$ and $c_z(\alpha)$ were derived from data in Ref. 4. The coefficients are:

$$c_x = 5.86689 \text{ e-}7 (\alpha)^3 - 6.72027 \text{ e-}5 (\alpha)^2 + .00332044 (\alpha) - .009534$$

$$c_z = -9.25704 \text{ e-}5 (\alpha)^2 + .0523808 (\alpha) - .832122$$

where α = angle of attack. These coefficients are used in the model to calculate a density derived from normal- and axial-acceleration measurements. The expected result, verifying the in-flight calibration technique, is that these densities derived from separate measurements are equal. Figures 5-16 profile the ratio of the densities derived from the axial and normal accelerations. The density results of flights STS-51F and STS-61A have unresolved anomalies. These anomalies have been noted and discussed in a previous analysis (see Ref. 1). A comparison of density ratios were performed between the values in Ref. 1 and the results obtained here. The mean of each density ratio was calculated from 80 to 140 km. The deviation of each mean is presented in Table V. The results from this new analysis show smaller deviations overall. Therefore, the current in-flight calibration technique has improved the analysis of HiRAP data.

Summary

There are time intervals during OV reentry when the aerodynamic acceleration level is known to be less than $1 \mu g$. Since ground calibration techniques may predict accelerations of $\pm 100 \mu g$ (or more), flight calibrations techniques are used to calibrate the HiRAP acceleration data.

The improvements to the in-flight calibration method have produced accelerations levels that are within $\pm 5.7 \mu g$ of zero for all HiRAP mission data sets. These calibrated data sets are used in the aerodynamic performance characteristics. The model calculates normal- and axial-densities from normal- and axial-accelerations, respectively. The results obtained here, compared with previous results, confirm that the changes to the in-flight calibration technique are indeed improvements.

References

- (1) Blanchard, R. C., Larman, K. T., and Barrett, M., "The High Resolution Accelerometer Package (HiRAP) Flight Experiment Summary for the First Ten Flights," NASA RP-1267, March 1992.
- (2) Blanchard, R. C., Larman, K. T., and Moats, C. D., "Ground and Flight Calibration Assessment of HiRAP Accelerometer Data from Missions STS-35 and STS-40," NASA TM - 107602, April 1992.
- (3) Blanchard, R. C., Hendrix, M. K., Fox, J. C., Thomas, D. J., and Nicholson, J. Y., "The Orbital Acceleration Research Experiment." Journal of Spacecrafts and Rockets, Vol. 24, No. 6, Nov. -Dec. 1987, pp. 504-511.
- (4) Aerodynamic Design Data Book. Volume 1 - Orbiter Vehicle, 1978; Part 1, NASA CR - 171859, 1978 (revised Sept. 1991). Part 2, NASA CR - 171854, 1978 (revised Sept. 1991).

Table I. HIRAP Calibration Parameters

Flight Number	Calibration Intervals (GMT, sec)		Altitudes (km)		Sensor Temperatures (°F)		APU Signal Shift (µg)
	X-axis	Z-axis	X-axis	Z-axis	X-axis	Z-axis	
STS-06	65200-65400	65250-65400	269.69-248.14	264.88-248.14	125.13-125.80	124.80-125.21	39
STS-07	47400-47710	47350-47556	266.67-227.65	271.73-248.55	70.47-72.04	69.45-70.47	40
STS-08	25030-25167	25140-25234	210.59-200.98	203.10-195.25	58.88-59.96	59.31-60.00	*
STS-09	82982-83123	83000-83142	215.24-202.62	213.76-200.76	89.95-91.05	89.71-90.88	*
STS-41B	41450-41600	41350-41519	245.52-228.55	255.08-238.10	51.12-52.20	49.90-51.06	41
STS-41C	46600-46800	46661-46830	291.46-237.20	274.89-229.15	72.73-73.82	72.37-73.25	*
STS-51B	55600-55850	55780-55910	290.56-286.29	250.16-223.96	64.01-65.37	64.05-64.80	*
STS-51F	68400-68690	68400-68521	273.55-228.02	273.55-255.85	73.28-74.59	72.48-73.02	21
STS-61A	61300-61450	61353-61572	254.41-227.40	245.12-204.11	98.77-99.32	98.47-99.44	*
STS-61C	47700-47897	47835-47966	261.25-228.57	239.24-216.38	107.16-107.93	107.24-107.76	*
STS-35	18501-18801	18501-18601	290.49-235.20	290.49-272.99	70.42-71.79	69.61-70.06	34
STS-40	53455-53706	53455-53706	275.70-245.16	275.70-245.16	67.68-68.84	66.89-68.04	37

* For these flights, a pre-APU calibration was not necessary.

Table II. HIRAP Calibration Results

Flight Number	Bias Slope ($\mu\text{g}/^\circ\text{F}$)		Bias Intercept (μg)		Calibration Uncertainty (μg)		
	X-axis	Z-axis	X-axis	Z-axis	X-axis	Z-axis	
STS-06	-23.28	-14.44	-1415.73	-1593.71	$\pm 1.42(\mu\text{g}/^\circ\text{F}) \pm 0.55\mu\text{g}$	$\pm 4.15(\mu\text{g}/^\circ\text{F}) \pm 2.29\mu\text{g}$	$+0.78\mu\text{g}$
STS-07	-17.40	-16.42	-231.85	-606.07	$\pm 0.22(\mu\text{g}/^\circ\text{F}) \pm 0.19\mu\text{g}$	$\pm 1.30(\mu\text{g}/^\circ\text{F}) \pm 2.63\mu\text{g}$	
STS-08	-25.04	-24.88	26.54	-341.19	$\pm 0.60(\mu\text{g}/^\circ\text{F}) \pm 0.37\mu\text{g}$	$\pm 1.60\mu\text{g}$	$\pm 4.53(\mu\text{g}/^\circ\text{F}) \pm 1.66\mu\text{g}$
STS-09	-22.12	-12.51	-3088.72	-203.99	$\pm 1.11(\mu\text{g}/^\circ\text{F}) \pm 0.73\mu\text{g}$	$\pm 1.02\mu\text{g}$	$\pm 2.82(\mu\text{g}/^\circ\text{F}) \pm 2.02\mu\text{g}$
STS-41B	-25.13	-23.70	162.20	-180.80	$\pm 0.39(\mu\text{g}/^\circ\text{F}) \pm 0.25\mu\text{g}$		$\pm 0.35(\mu\text{g}/^\circ\text{F}) \pm 2.84\mu\text{g}$
STS-41C	-18.52	-16.49	-328.13	-634.90	$\pm 0.95(\mu\text{g}/^\circ\text{F}) \pm 0.59\mu\text{g}$		$\pm 2.00(\mu\text{g}/^\circ\text{F}) \pm 1.01\mu\text{g}$
STS-51B	-21.93	-18.60	-270.00	-584.33	$\pm 0.55(\mu\text{g}/^\circ\text{F}) \pm 0.46\mu\text{g}$		$\pm 2.69(\mu\text{g}/^\circ\text{F}) \pm 1.25\mu\text{g}$
STS-51F	-17.75	-9.57	5457.62	5463.83	$\pm 0.55(\mu\text{g}/^\circ\text{F}) \pm 0.42\mu\text{g}$		$\pm 1.41(\mu\text{g}/^\circ\text{F}) \pm 1.40\mu\text{g}$
STS-61A	-19.66	-8.76	4949.13	5192.69	$\pm 1.62(\mu\text{g}/^\circ\text{F}) \pm 0.59\mu\text{g}$		$\pm 2.21(\mu\text{g}/^\circ\text{F}) \pm 1.14\mu\text{g}$
STS-61C	-25.06	-12.80	-2019.08	-1764.45	$\pm 3.25(\mu\text{g}/^\circ\text{F}) \pm 1.55\mu\text{g}$		$\pm 5.26(\mu\text{g}/^\circ\text{F}) \pm 1.65\mu\text{g}$
*STS-35	-24.56	-22.88	682.72	-1280.00	$\pm 1.44(\mu\text{g}/^\circ\text{F}) \pm 0.82\mu\text{g}$		$\pm 1.93(\mu\text{g}/^\circ\text{F}) \pm 1.03\mu\text{g}$
STS-40	-25.05	-21.98	726.90	-1257.80	$\pm 0.95(\mu\text{g}/^\circ\text{F}) \pm 0.61\mu\text{g}$		$\pm 0.58(\mu\text{g}/^\circ\text{F}) \pm 1.49\mu\text{g}$

* The analysis of STS-35 was redone to minimize the amount of data lost due to thrust removal. Therefore, the results documented here vary slightly from those in Reference 2.

Table III. Maximum Orbital Acceleration Measurement Uncertainties

Flight Number	X-axis (μg)	Z-axis (μg)
STS-06	1.50	4.77
STS-07	0.54	3.96
STS-08	2.62	5.65
STS-09	2.97	5.32
STS-41B	0.67	3.25
STS-41C	1.63	2.77
STS-41C	1.21	3.27
STS-51B	1.14	2.16
STS-61A	1.48	4.28
STS-61C	4.05	4.39
STS-35	2.79	1.90
STS-40	1.71	2.16

Table IV. Maximum Reentry Acceleration Measurement Uncertainty

Flight Number	X-axis (μg)	Z-axis (μg)
STS-06	6.23	17.23
STS-07	1.49	10.13
STS-08	6.08	26.40
STS-09	8.57	19.06
STS-41B	2.54	5.74
STS-41C	4.79	8.24
STS-51B	3.41	11.91
STS-51F	3.29	8.00
STS-61A	7.03	10.67
STS-61C	14.42	18.32
STS-35	8.02	10.37
STS-40	5.69	4.45

Table V. % Deviation from Equal Densities

Flight Number	Current Analysis	Reference 1 Analysis
STS-06	+0.57	+2.50
STS-07	-1.00	+7.72
STS-08	+2.76	+6.86
STS-09	+5.80	+18.17
STS-41B	-0.05	+5.18
STS-41C	+0.04	+2.37
STS-51B	+0.96	-1.92
† STS-51F	+8.50	+1.68
† STS-61A	+6.49	+3.63
STS-61C	+1.55	-4.61
STS-35	+4.42	*
STS-40	+6.38	*

*Flight was only evaluated with current flight calibration technique.

†The density results are in error. The analysis of this error can be found in Reference 1.

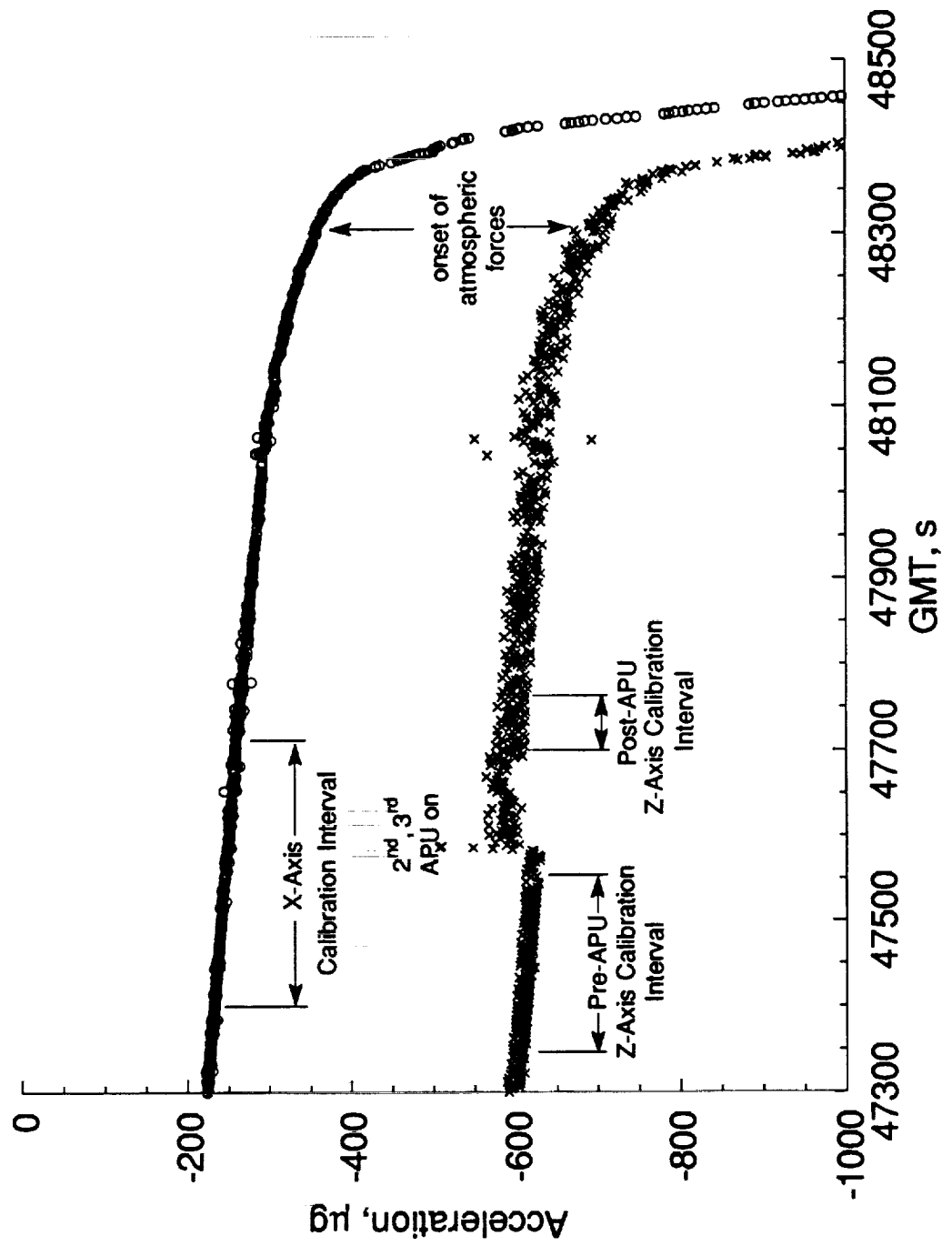


Figure 1. HiRAP STS-07 Uncalibrated Flight Data.

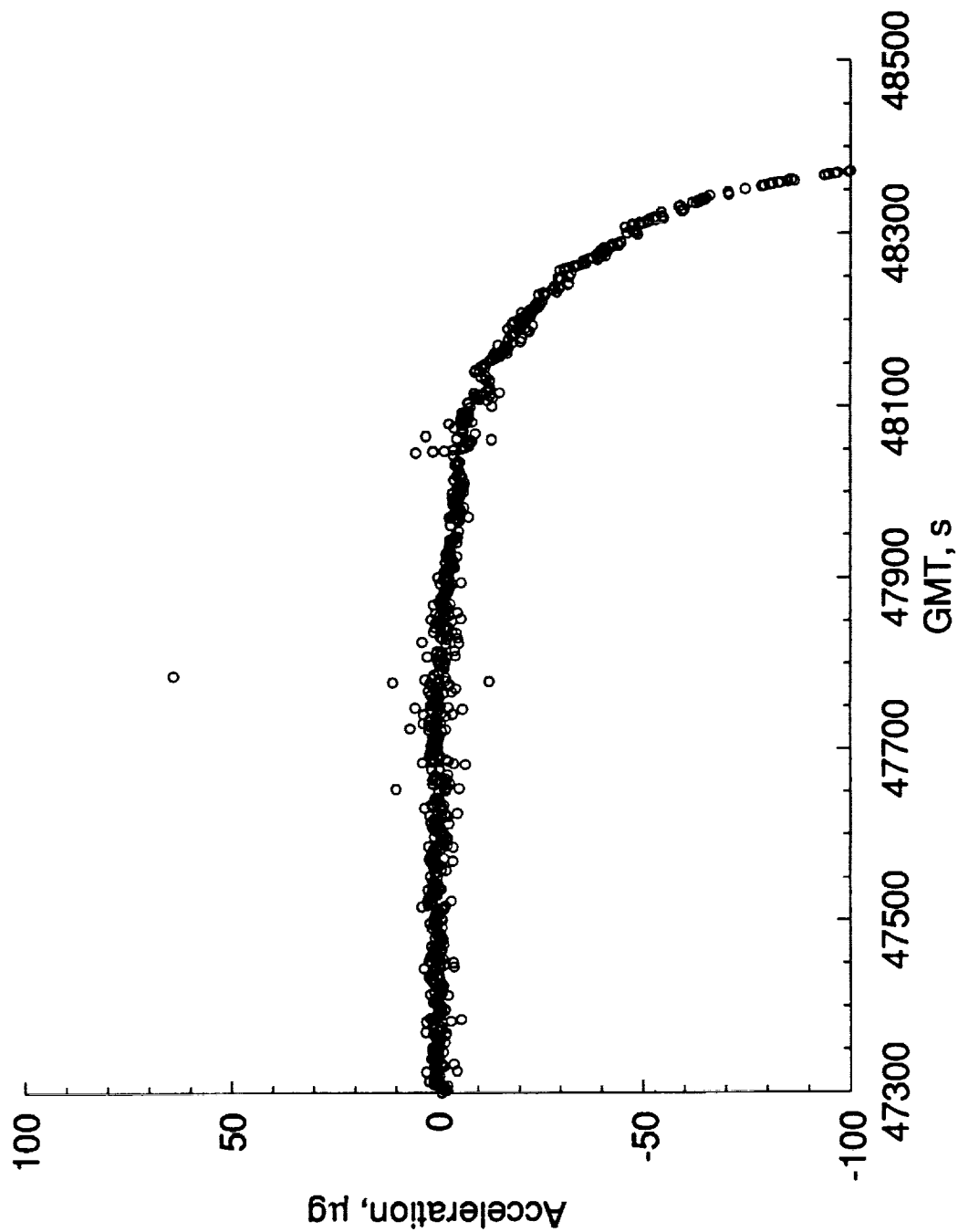


Figure 2. HIRAP ST-07 Flight Calibrated X-Axis Data.

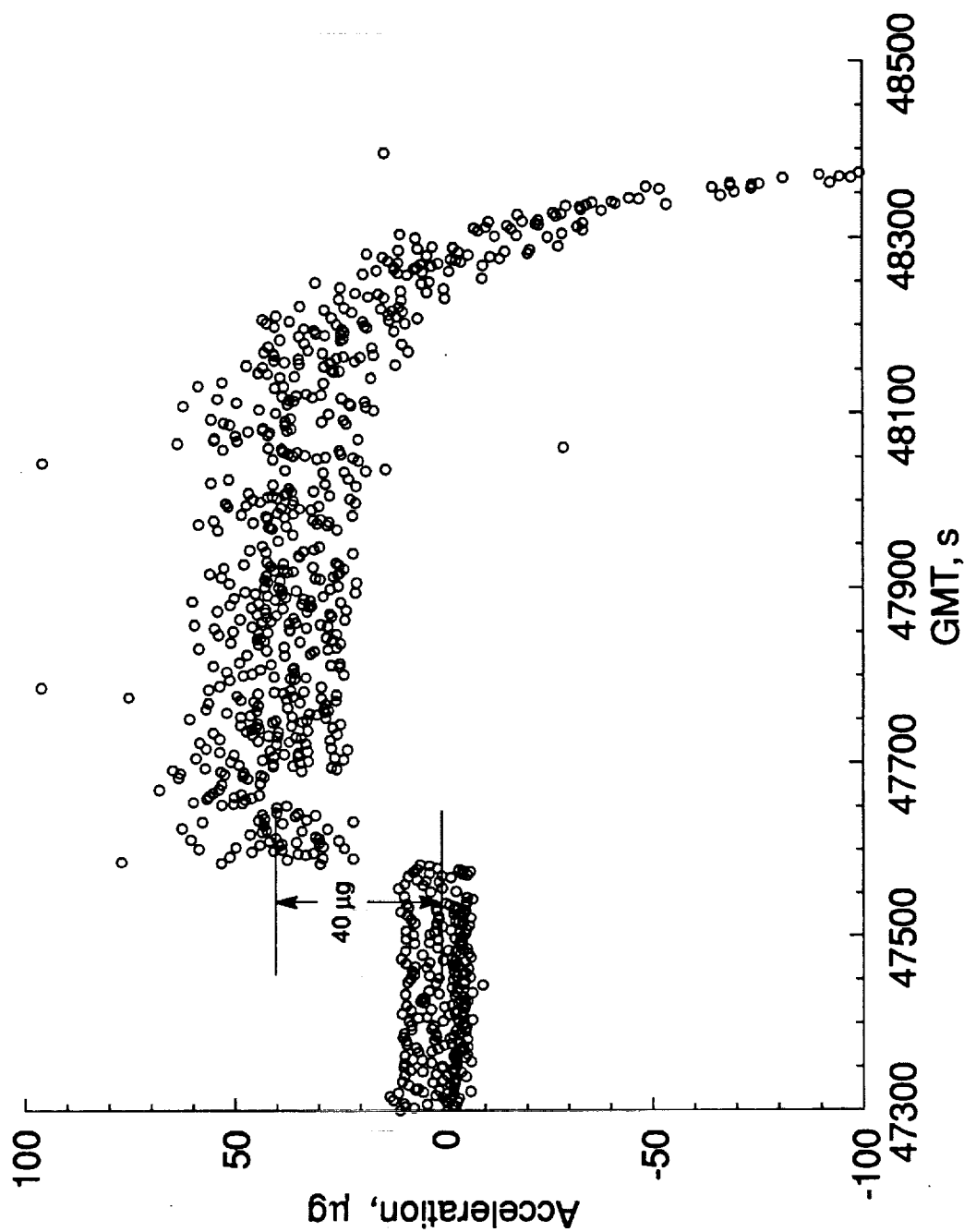


Figure 3. HiRAP STS-07 Calibrated Z-Axis Data.

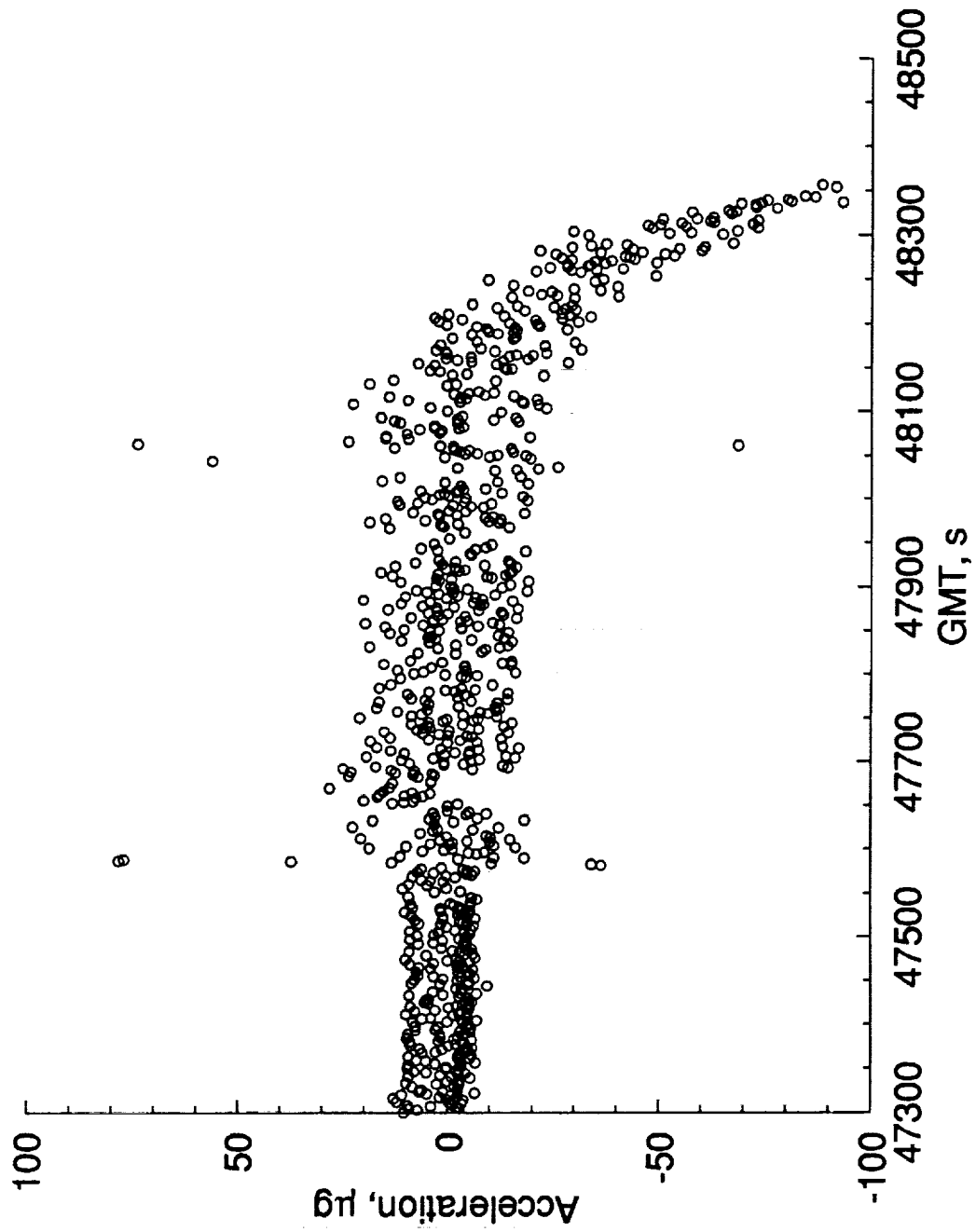


Figure 4. HiRAP STS-07 Flight Calibrated Z-Axis Data with APU Correction.

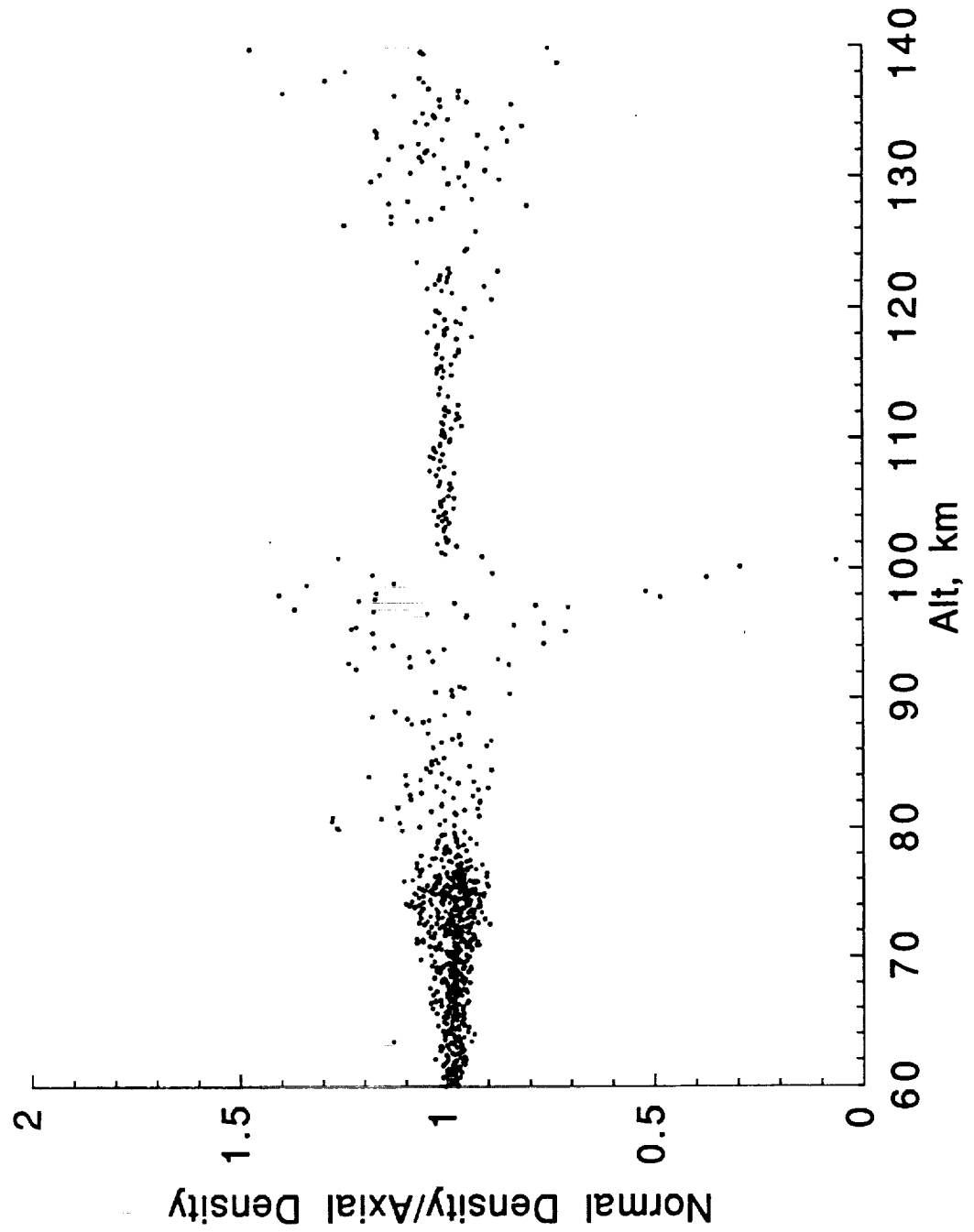


Figure 5. HiRAP STS-06.

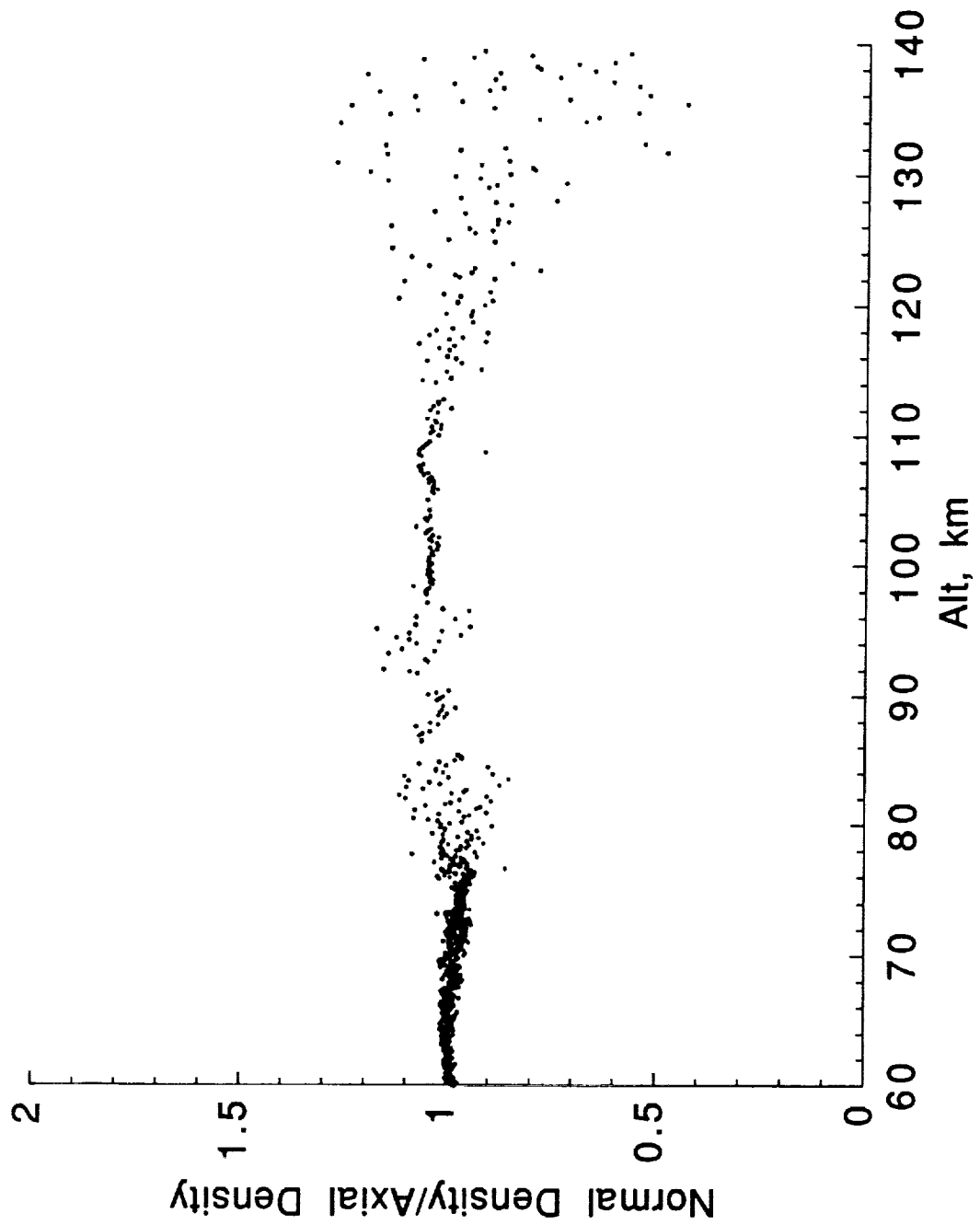


Figure 6. HiRAP STS-07.

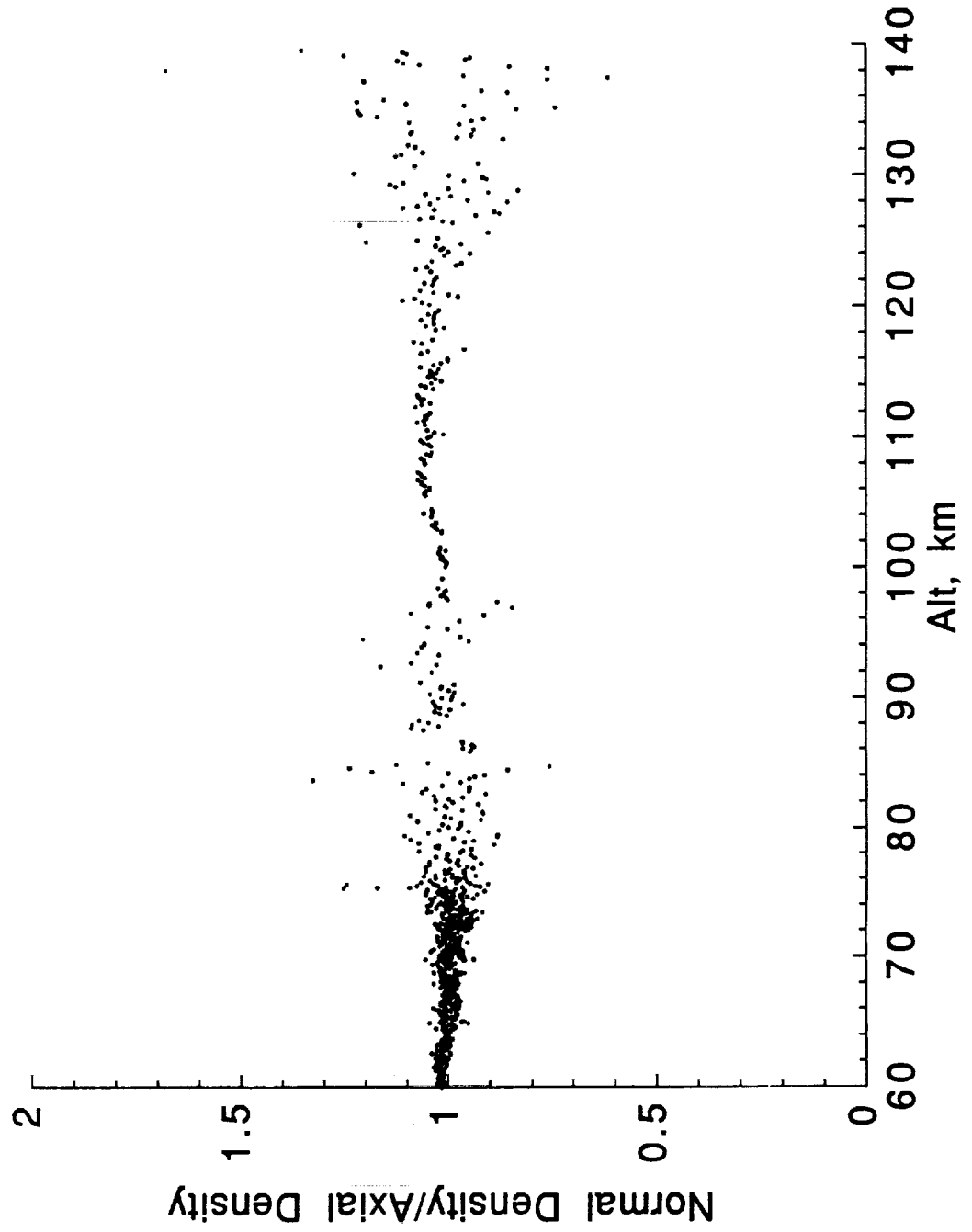


Figure 7. HiRAP STS-08.

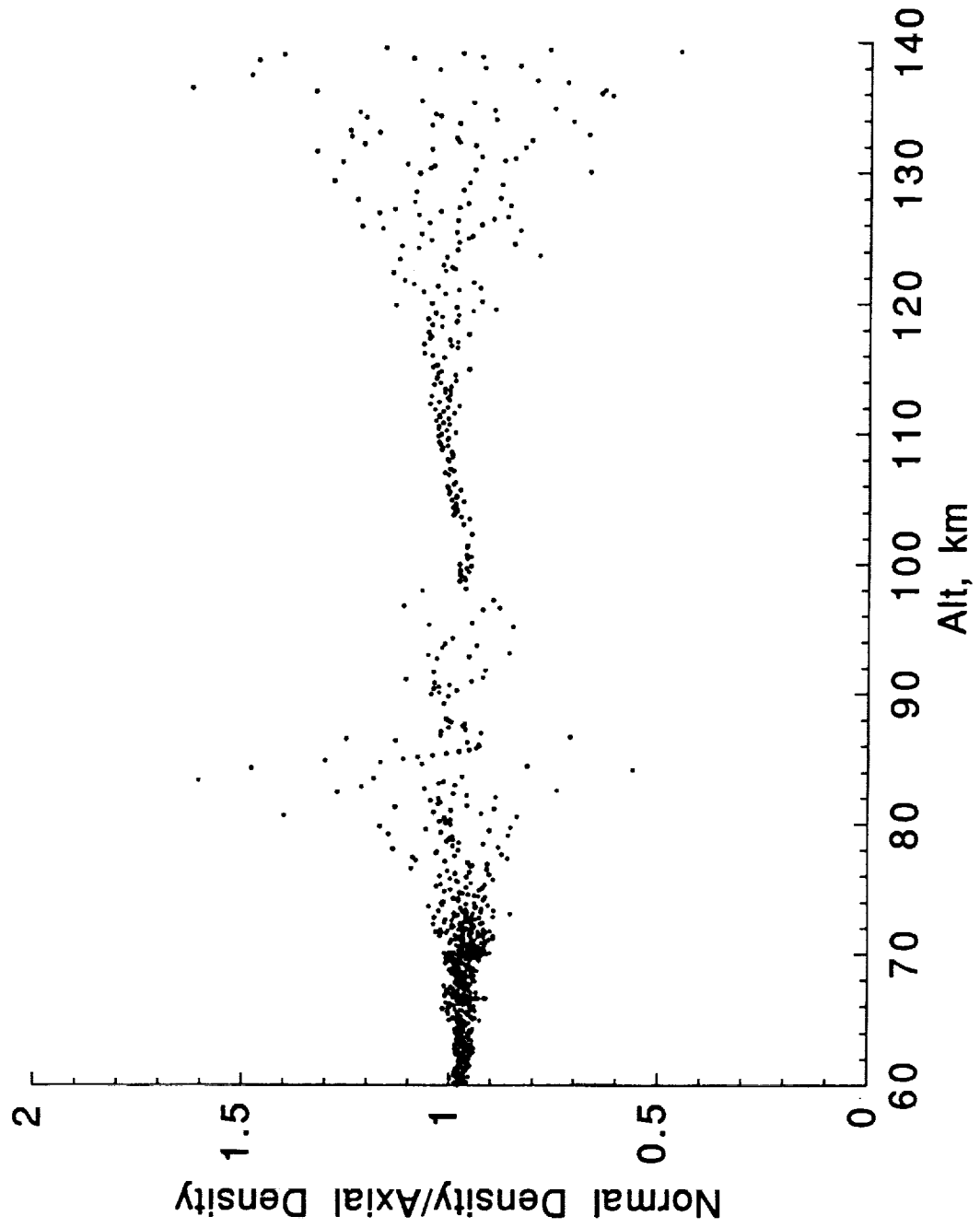


Figure 8. HiRAP STS-09.

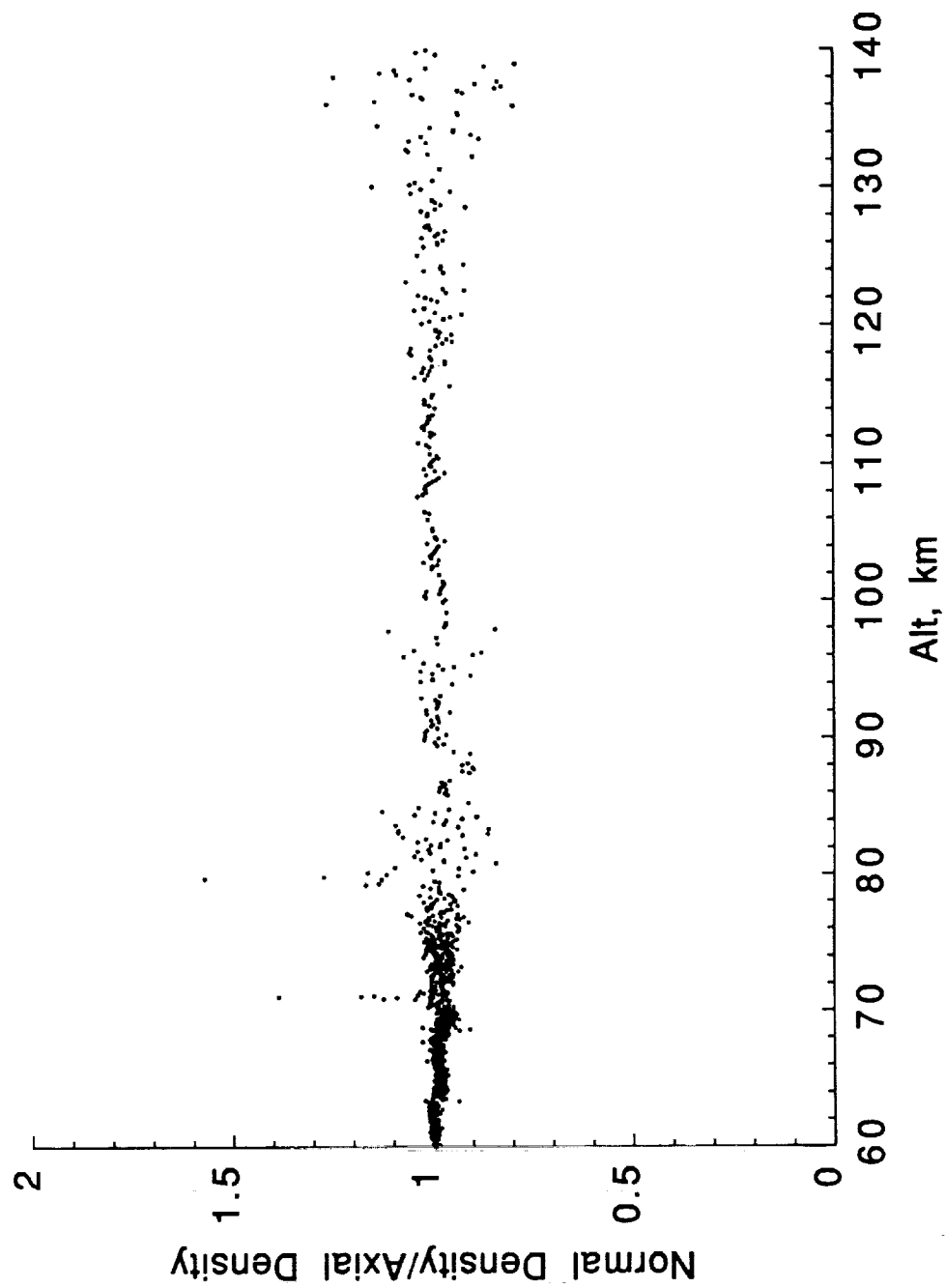


Figure 9. HIRAP STS-41B.

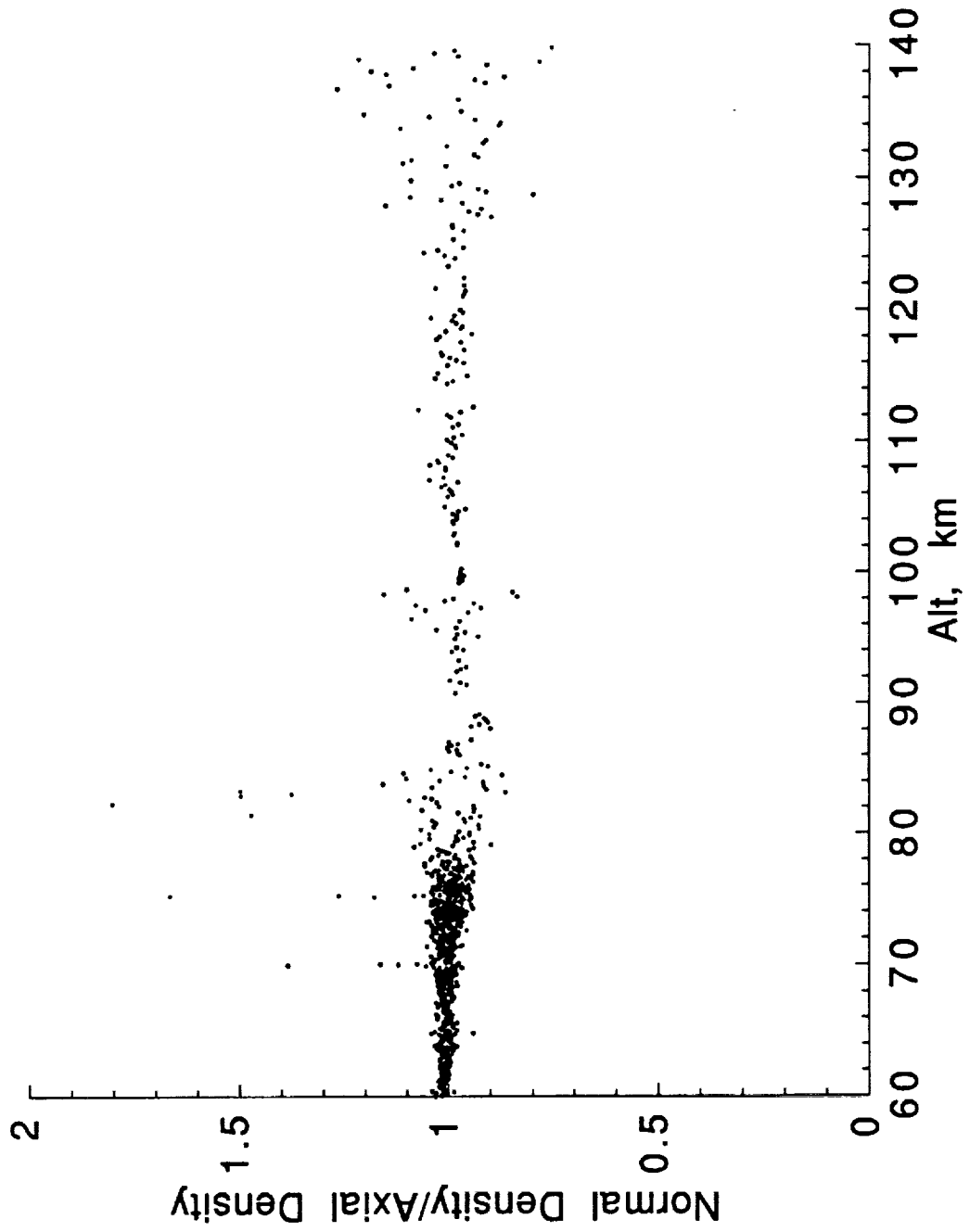


Figure 10. HiRAP STS-41C.

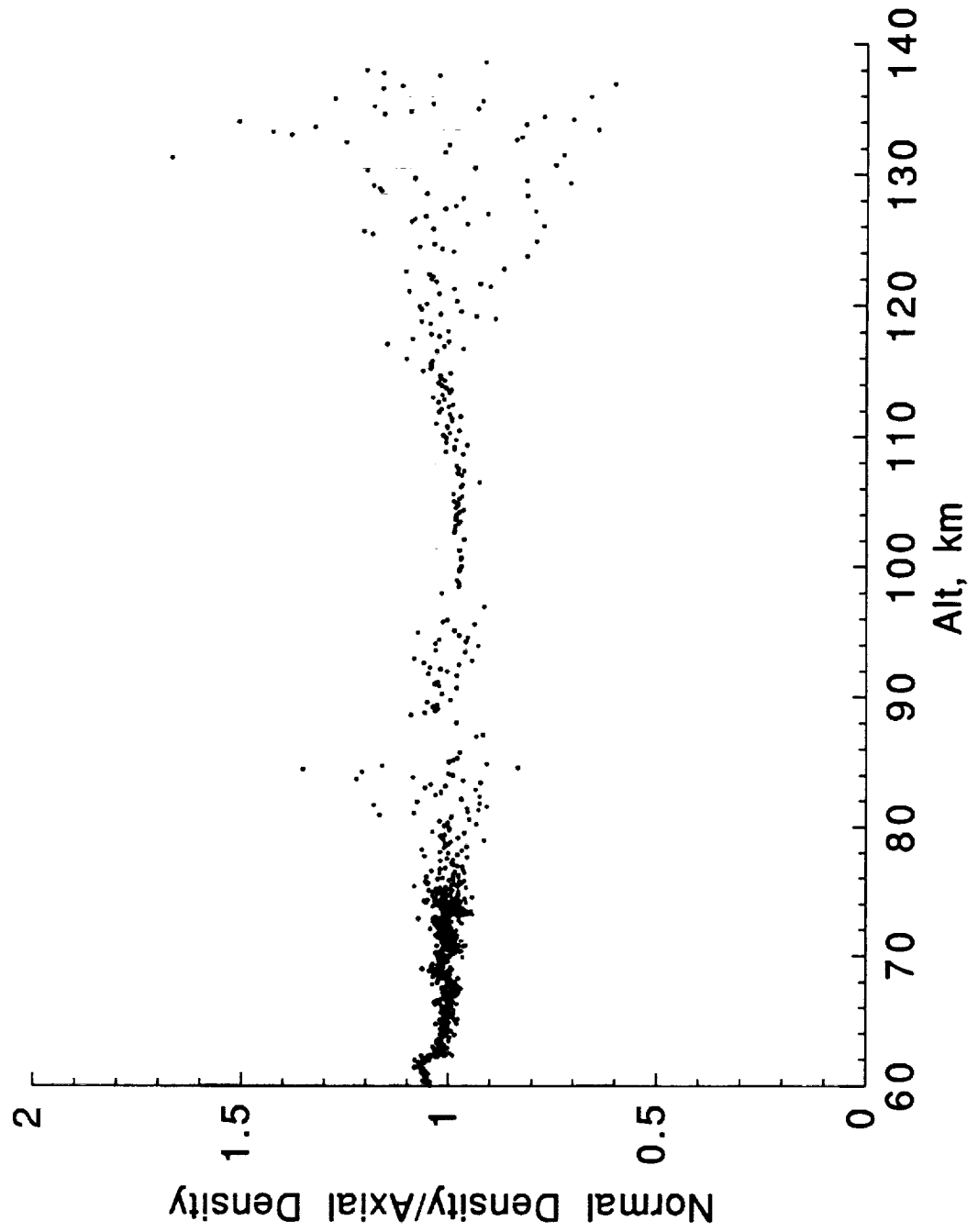


Figure 11. HiRAP STS-51B.

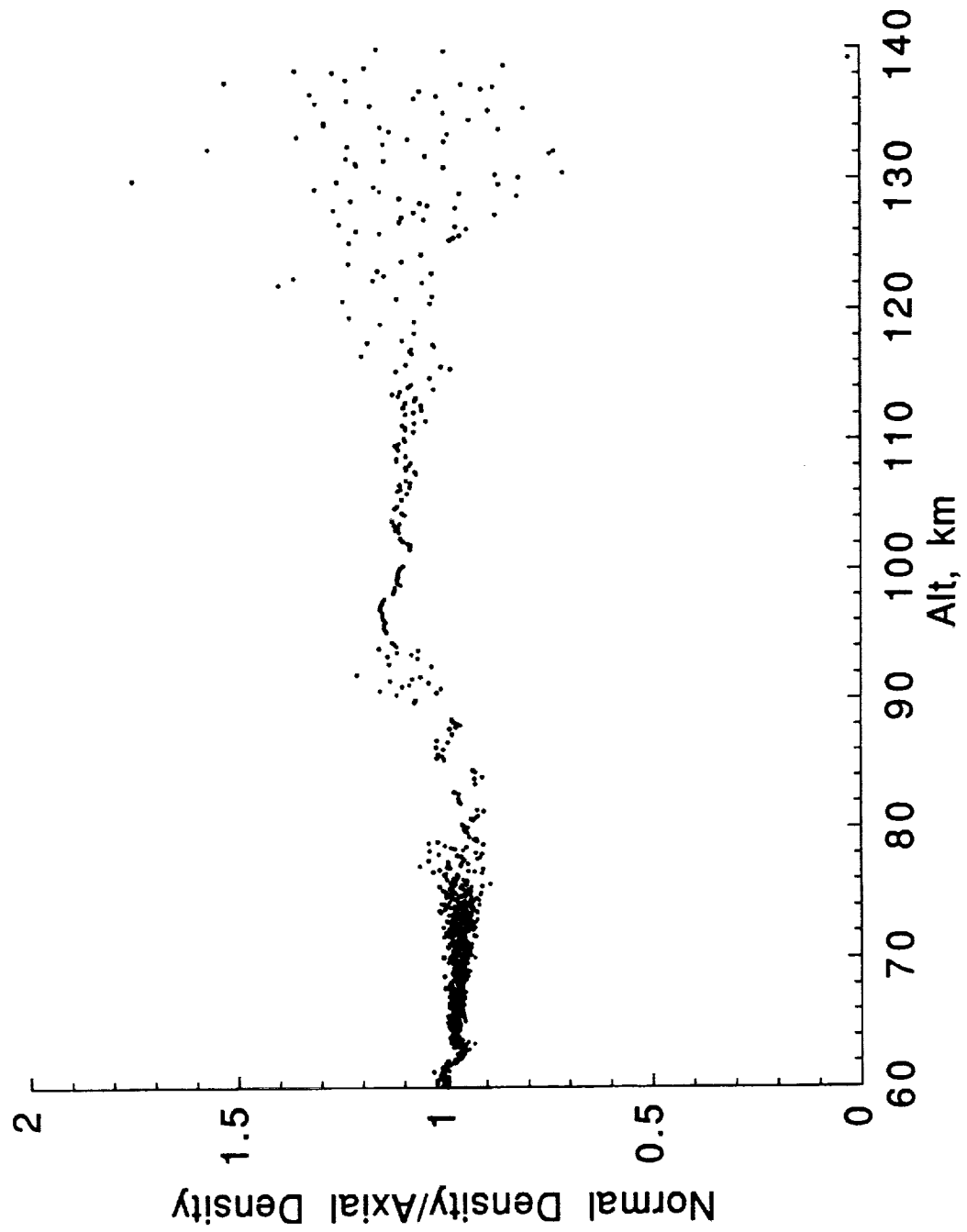


Figure 12. HiRAP STS-51F.

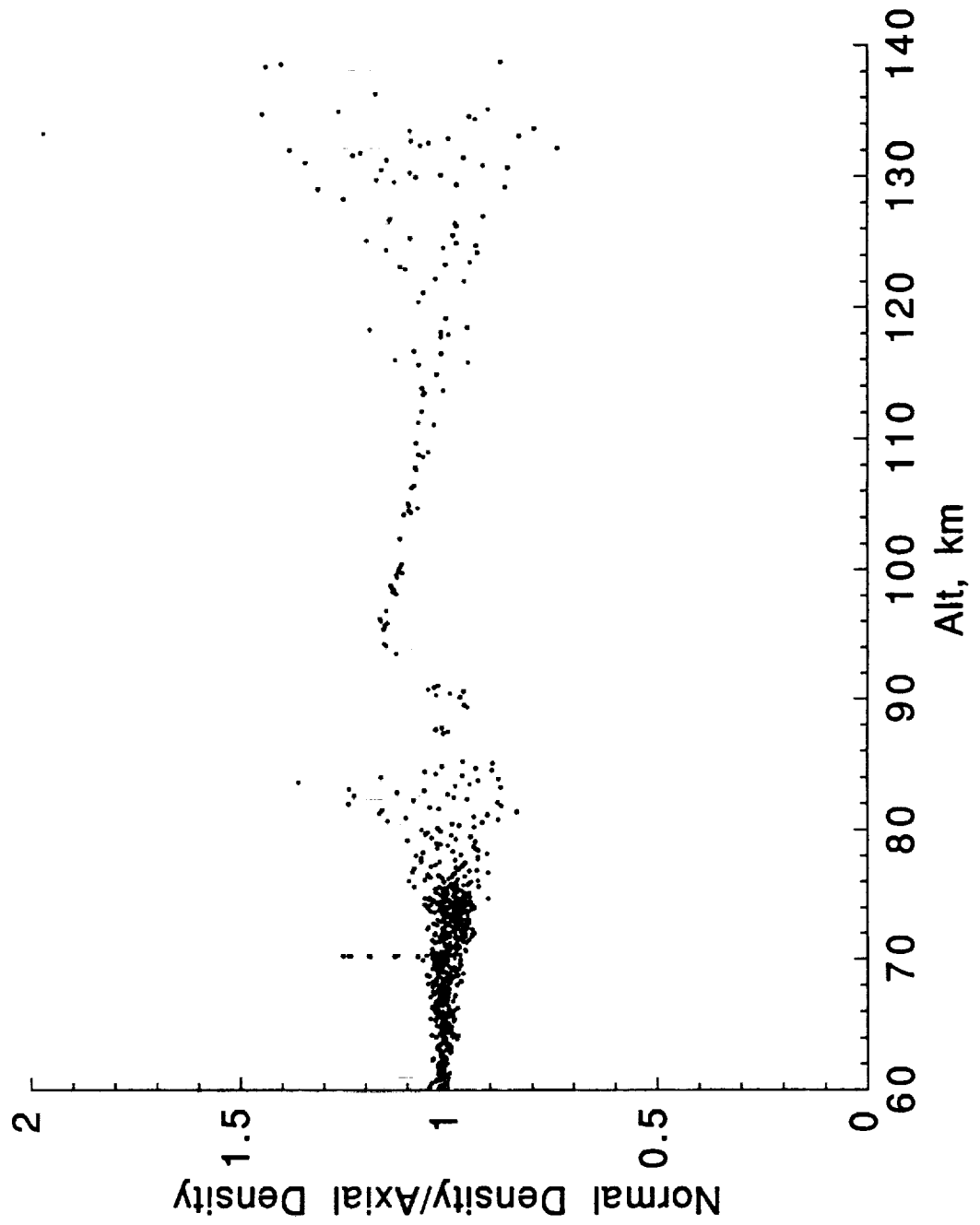


Figure 13. HiRAP STS-61A.

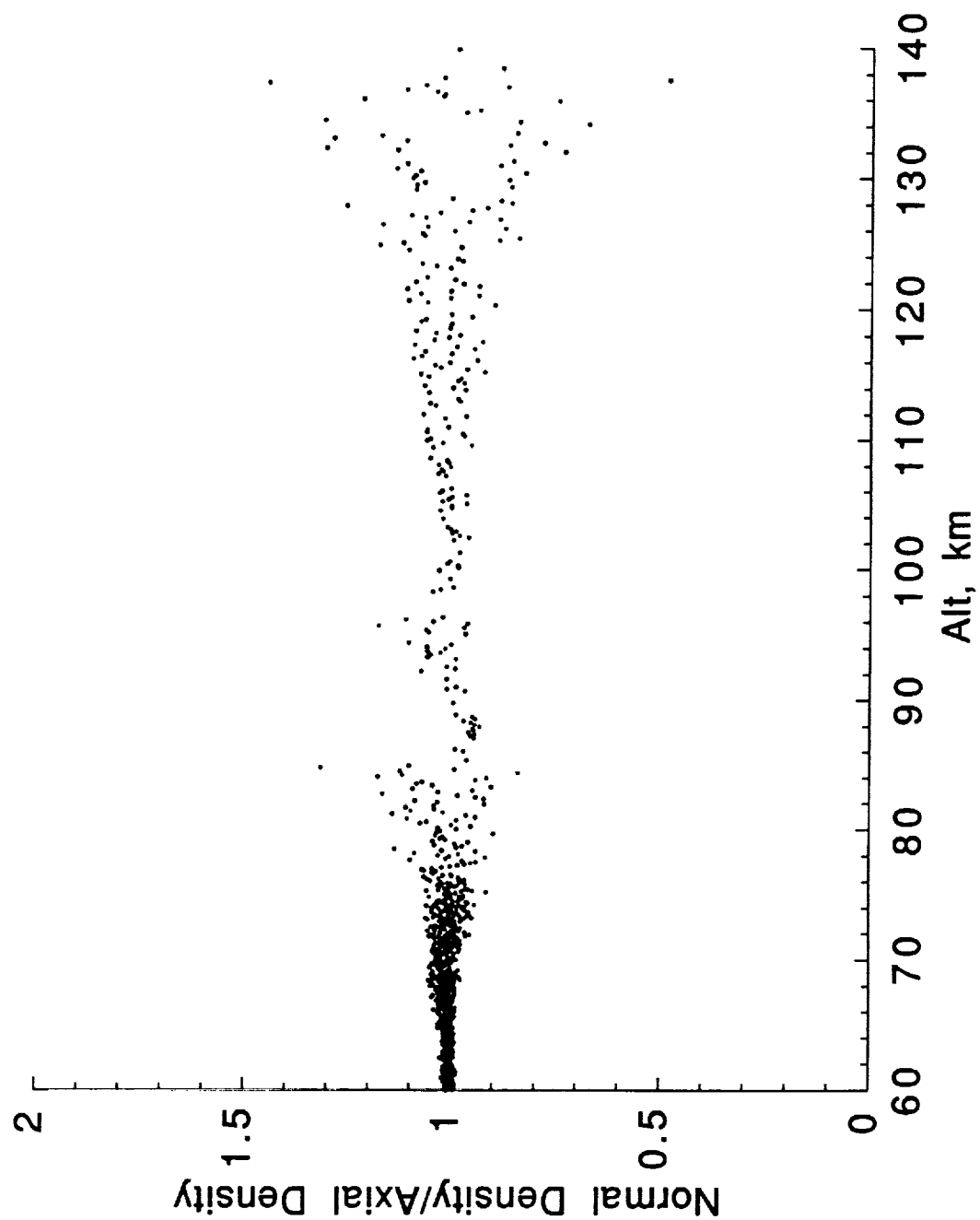


Figure 14. HiRAP STS-61C.

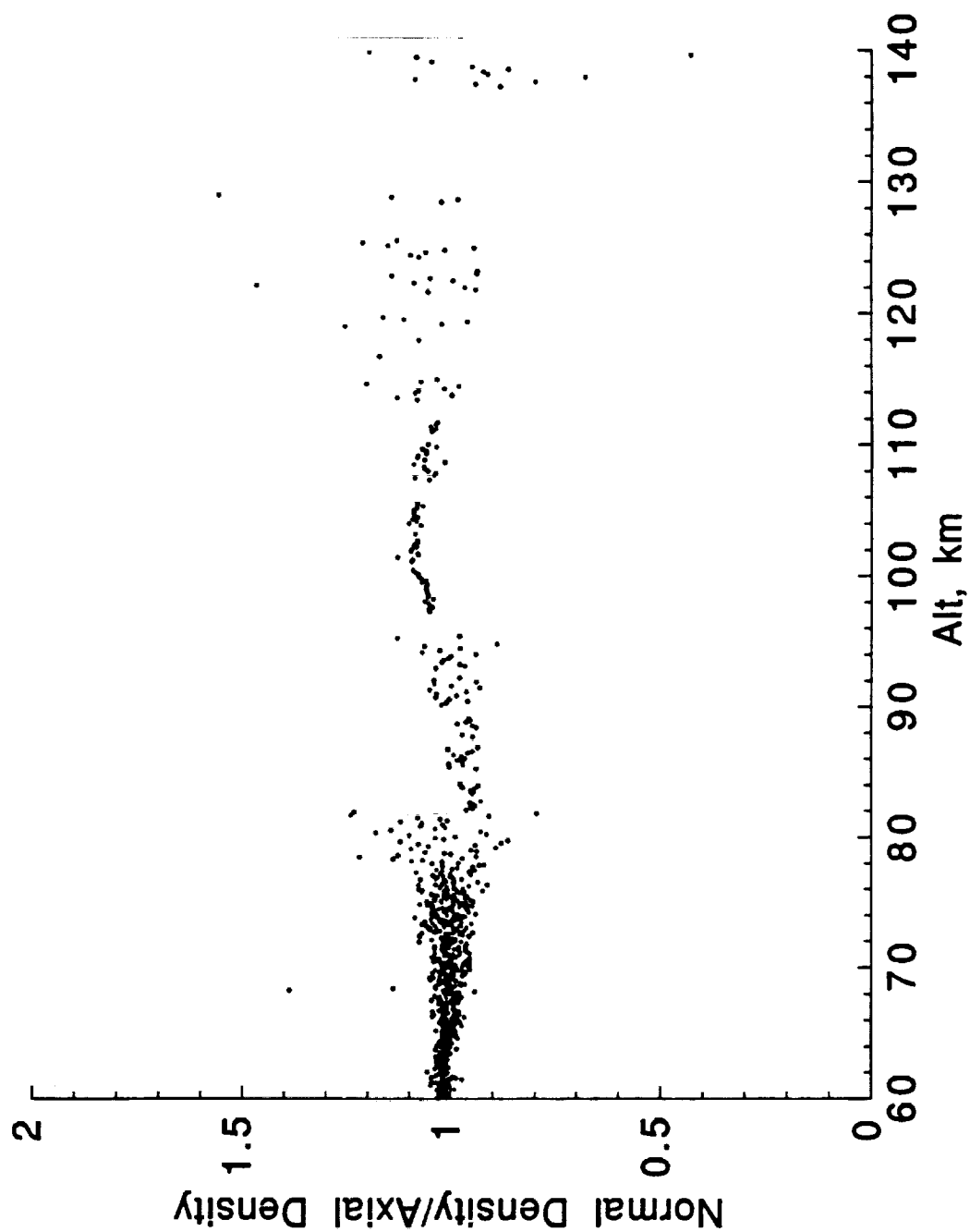


Figure 15. HIRAP STS-35.

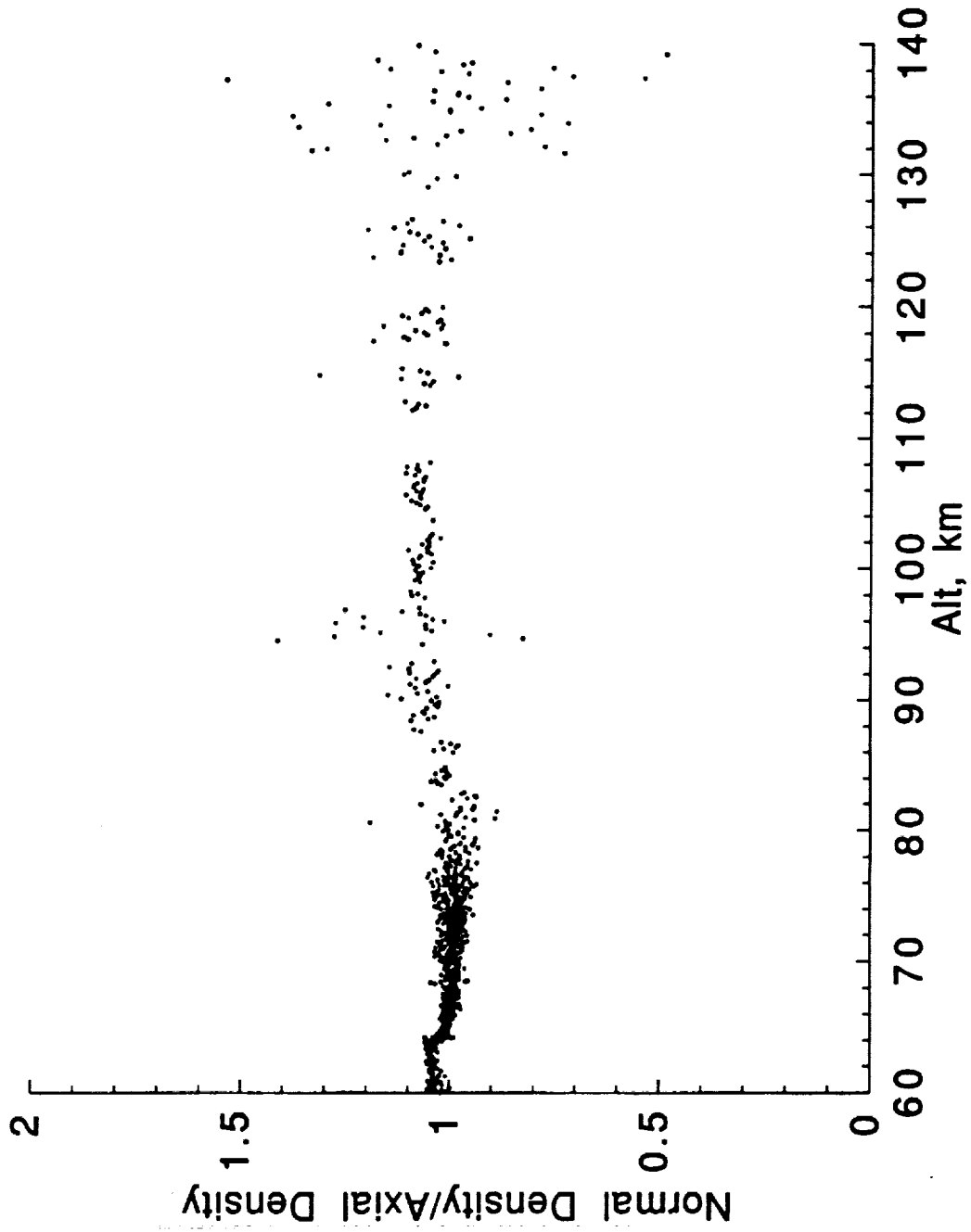


Figure 16. HiRAP STS-40.

REPORT DOCUMENTATION PAGE

Form Approved
OMB No. 0704-0188

Public reporting burden for this collection of information is estimated to average 1 hour per response, including the time for reviewing instructions, searching existing data sources, gathering and maintaining the data needed, and completing and reviewing the collection of information. Send comments regarding this burden estimate or any other aspect of this collection of information, including suggestions for reducing this burden, to Washington Headquarters Services, Directorate for Information Operations and Reports, 1215 Jefferson Davis Highway, Suite 1204, Arlington, VA 22202-4302, and to the Office of Management and Budget, Paperwork Reduction Project (0704-0188), Washington, DC 20503

1. AGENCY USE ONLY (Leave blank)		2. REPORT DATE July 1992	3. REPORT TYPE AND DATES COVERED Technical Memorandum	
4. TITLE AND SUBTITLE Improved HiRAP Flight Calibration Technique			5. FUNDING NUMBERS WU 506-48-11-04	
6. AUTHOR(S) Christina D. Moats, Robert C. Blanchard, and Kevin T. Larman				
7. PERFORMING ORGANIZATION NAME(S) AND ADDRESS(ES) NASA Langley Research Center Hampton, VA 23665-5225			8. PERFORMING ORGANIZATION REPORT NUMBER	
9. SPONSORING/MONITORING AGENCY NAME(S) AND ADDRESS(ES) National Aeronautics and Space Administration Washington, DC 20546-0001			10. SPONSORING/MONITORING AGENCY REPORT NUMBER NASA TM-107656	
11. SUPPLEMENTARY NOTES Moats and Larman: Lockheed Engineering & Sciences Company, Hampton, Virginia. Blanchard: Langley Research Center, Hampton, Virginia.				
12a. DISTRIBUTION/AVAILABILITY STATEMENT Unclassified-Unlimited Subject Category 19			12b. DISTRIBUTION CODE	
13. ABSTRACT (Maximum 200 words) A method of removing non-aerodynamic acceleration signals and calibrating the High Resolution Accelerometer Package (HiRAP) has been developed and improved. Twelve HiRAP mission data sets have been analyzed applying the improved in-flight calibration technique. The application of flight calibration factors to the data sets from these missions produced calibrated acceleration levels within $\pm 5.7 \mu g$ of zero during a time in-flight when the acceleration level was known to be less than 1 g. To validate the current in-flight calibration technique, the atmospheric density results, specifically the normal-to-axial density ratios, have been compared with the analysis results obtained with the previous in-flight calibration technique. This comparison shows an improvement (up to 12.4 percent per flight) in the density ratio when the updated in-flight calibration technique is used.				
14. SUBJECT TERMS Micro-gravity acceleration, calibration, and reentry			15. NUMBER OF PAGES 27	
			16. PRICE CODE A03	
17. SECURITY CLASSIFICATION OF REPORT Unclassified	18. SECURITY CLASSIFICATION OF THIS PAGE Unclassified	19. SECURITY CLASSIFICATION OF ABSTRACT	20. LIMITATION OF ABSTRACT	